ACTIVATION OF THE WNT/β-CATENIN SIGNALING CASCADE AFTER TRAUMATIC NERVE INJURY

S. KURIMOTO[a,g], **J. JUNG**[a], **M. TAPADIA**[a], **J. LENGFELD**[b], **D. AGALLIU**[b], **M. WATERMAN**[c], **T. MOZAFFAR**[a,d], and **R. GUPTA**[a,e,f,*]

[a]Department of Orthopaedic Surgery, University of California, Irvine, CA 92697, USA

[b]Department of Developmental and Cell Biology, University of California, Irvine, CA 92697, USA

[c]Department of Microbiology and Molecular Genetics, University of California, Irvine, CA 92697, USA

[d]Department of Neurology, University of California, Irvine, CA 92697, USA

[e]Department of Biomedical Engineering, University of California, Irvine, CA 92697, USA

[f]Department of Anatomy and Neurobiology, University of California, Irvine, CA 92697, USA

[g]Department of Hand Surgery, Nagoya University Graduate School of Medicine, 65 Tsurumai-Cho, Showa-Ku, Nagoya 466-8550, Japan

Abstract

Recent data have shown that preservation of the neuromuscular junction (NMJ) after traumatic nerve injury helps to improve functional recovery with surgical repair via matrix metalloproteinase-3 (MMP3) blockade. As such, we sought to explore additional pathways that may augment this response. Wnt3a has been shown to inhibit acetylcholine receptor (AChR) clustering via β-catenin-dependent signaling in the development of the NMJ. Therefore, we hypothesized that Wnt3a and β-catenin are associated with NMJ destabilization following traumatic denervation. A critical size nerve defect was created by excising a 10-mm segment of the sciatic nerve in mice. Denervated muscles were then harvested at multiple time points for immunofluorescence staining, quantitative real-time PCR, and western blot analysis for Wnt3a and β-catenin levels. Moreover, a novel Wnt/β-catenin transgenic reporter mouse line was utilized to support our hypothesis of Wnt activation after traumatic nerve injury. The expression of Wnt3a mRNA was significantly increased by 2 weeks post-injury and remained upregulated for 2 months. Additionally, β-catenin was activated at 2 months post-injury relative to controls. Correspondingly, immunohistochemical analysis of denervated transgenic mouse line TCF/Lef:H2B-GFP muscles demonstrated that the number of GFP-positive cells was increased at the motor endplate band. These collective data support that post-synaptic AChRs destabilize after denervation by a process that involves the Wnt/β-catenin pathway. As such, this pathway serves as a potential therapeutic target to prevent the motor endplate degeneration that occurs following traumatic nerve injury.

[*]Correspondence to: R. Gupta, Department of Orthopaedic Surgery, University of California, Irvine, 2226 Gillespie Neurosciences Research Facility, Irvine, CA 92697, USA. Tel: +1-949-824-1405; fax: +1-949-824-1462. ranjang@uci.edu (R. Gupta).

Keywords

peripheral nerve; Wnt signaling; traumatic nerve injury; neuromuscular junction

INTRODUCTION

While the peripheral nervous system has the capacity for regeneration following injury, clinicians are acutely aware that functional recovery after peripheral nerve injuries is quite limited in adults. There has been a proliferation of strategies to enhance the ability of axons to bridge the injury gap in recent decades (Ray and Mackinnon, 2010). However, these modern advances in surgical treatment based on anatomic reconstruction, autografting, and peripheral nerve guides have reached a plateau in terms of the optimal functional outcomes that are possible (Kang et al., 2011; Griffin et al., 2013). Even with optimal medical and surgical management of their nerve injury, muscle function is only partially restored and muscle strength and dexterity never completely recovers to the pre-injury state (Bentolila et al., 1999; Kim et al., 2003; Kang et al., 2011). This is especially true with proximal major nerve injuries. One reason for this phenomenon may be explained by degeneration or atrophy of target end organs (Tung and Mackinnon, 2010). Nerve injuries that are treated with primary repair regenerate at a rate of approximately 1 mm per day and axons are usually unable to reach their targets before denervation-induced changes occur in the muscle (Seddon et al., 1943). Long-term denervation leads to profound atrophy in end-plate structure (Chao et al., 2013). Clinicians treating peripheral nerve injuries widely recognize that a further understanding of the molecular biology of peripheral nerve injury and repair is required to improve treatments for major nerve injuries.

Neuromuscular junction (NMJ) formation during development requires neuronal agrin, a factor released from motoneurons which activates the tyrosine kinase muscle-specific kinase (MuSK) via low-density lipoprotein receptor-related protein 4 (Lrp4) (McMahan, 1990; Valenzuela et al., 1995; Zhang et al., 2008). By contrast, acetylcholine released from the motoneuron to acetylcholine receptors (AChRs) elicits a negative pathway to disassemble the postsynaptic apparatus (Lin et al., 2005). These dynamic interactions between positive and negative signals are thought to be necessary to regulate AChR clusters and allow for their proper functioning.

Recently, Wnt signaling proteins have been shown to augment both synaptogenic and anti-synaptogenic functions in the development of the NMJ (Henríquez and Salinas, 2012). Wnt is a family of secreted signaling proteins with various developmental functions ranging from morphogenesis, cell proliferation, and cell survival (Clevers and Nusse, 2012). Wnts are coupled to various receptors and thereby activate different downstream pathways. These pathways have been classified as either canonical (β-catenin dependent) or non-canonical (β-catenin independent) signaling pathways. β-Catenin is a key target of the canonical Wnt pathway, and it mediates many cellular processes in response to Wnt (Niehrs, 2012). Upregulation of canonical Wnts leads to the activation and nuclear translocation of β-catenin through inhibition of the β-catenin phospho-degradation complex, which in turn, regulates transcription of target genes (Moon et al., 2002; Li et al., 2012). Inhibitory roles of Wnts in

the development of the NMJ were supported by the finding that Wnt3a inhibits agrin-induced AChR clustering by suppressing rapsyn expression via the canonical β-catenin-dependent signaling pathway (Wang et al., 2008). During development, although agrin-induced AChR clustering and the ensuing formation of the NMJ was reduced by Wnt3a, it was enhanced by Wnt3. These Wnts preferentially activate β-catenin-dependent and β-catenin-independent pathways, respectively (Niehrs, 2012). Contrastingly, there are also positive regulators of AChR clustering that occurs via the non-canonical Wnt pathway. Recent data have implicated Wnt3 as a possible effector, which may bind directly to MuSK cysteine-rich domains to have its effects (Henriquez et al., 2008; Takamori, 2012). In the developmental stage, these dual roles of Wnts helps NMJ development and homeostasis during the formation of the vertebrate NMJ (Henriquez et al., 2008; Koles and Budnik, 2012; Samuel et al., 2012; Takamori, 2012).

Introduction of agrin into denervated muscles elicits formation of postsynaptic apparatus (Bezakova et al., 2001). We have recently provided the first evidence that preservation of the NMJ after traumatic nerve injury improves functional recovery after surgical repair (Chao et al., 2013). Matrix metalloproteinase-3 (MMP3) is a pro-tease, released from Schwann cells, that cleaves agrin in the synaptic cleft. By maintaining this agrin-mediated pathway via genetic deletion of MMP3, we were able to stabilize the motor endplate after injury. As the ensuing improvement in functional recovery was not to pre-injury level, we sought to explore additional pathways that may augment this response. As the role of the Wnt pathways in the maintenance of NMJs in skeletal muscle after denervation has not been previously explored, we hypothesized that Wnt3a and β-catenin are associated with NMJ destabilization following traumatic nerve injury.

EXPERIMENTAL PROCEDURES

Animal model

All procedures involving living animals were approved by the institutional animal care and use committee of the University of California, Irvine. Studies were conducted in male wild-type 129 Sv/Ev mice (gift from Dr. Wee Yong at the University of Calgary). Wnt/β-catenin signaling activity was studied using a transgenic mouse line (TCF/Lef:H2B-GFP, gift from Dr. Dritan Agalliu at the University of California, Irvine) expressing a fluorescent reporter for β-catenin-mediated canonical Wnt signaling (Ferrer-Vaquer et al., 2010). Briefly, upon Wnt binding of target receptors, β-catenin is then released from a degradation complex and translocates to the nucleus. There, β-catenin works together with the TCF/Lef family transcription factors and the heat shock promoter hsp68 to drive transcription of β-catenin-related genes to which GFP is linked. GFP thereby acts as a reporter for canonical pathway activation. Genotyping was performed by Transnetyx (Cordova, TN, USA).

For denervation studies, 6-week-old male animals from either wild-type or TCF/Lef:H2B-GFP mice were anesthetized with ketamine/xylazine. A critical size nerve defect was created by excising a 10-mm segment of the right sciatic nerve and the proximal nerve stump was sutured into hip muscles to prevent reinnervation. The gastroc–soleus complex and plantaris muscles were harvested at 1 week, 2 weeks, 1 month, and 2 months for various studies. The contralateral nerve of each animal was dissected, mobilized, and returned to the host bed to

serve as a control. Wnt3a and β-catenin levels were quantified via immunohistochemical staining, immunoblot analysis, and quantitative real-time PCR (qRT-PCR) to determine if NMJ destabilization is associated with increased concentration of these proteins within the motor endplate.

Quantitative real-time PCR

Whole gastroc–soleus complex harvested from wild-type ($n = 7$) was processed for RNA isolation using TRIzol reagent (Invitrogen, Carlsbad, CA, USA) according to the manufacturer's instructions and RNA concentrations were determined by using NanoDrop Lite (Thermo Scientific, Rockford, IL, USA). Reverse transcription was performed using 5-μg RNA of each total RNA sample with Transcriptor First Strand cDNA Synthesis Kit (Roche, Indianapolis, IN, USA). The cDNA of interest was amplified using the TaqMan Fast Advanced Master Mix and TaqMan Gene Expression assays (Wnt3a, Mm03053669_s1; Wnt3, Mm00437336_m1; 18 S rRNA, 4352930E) with a StepOnePlus real-time PCR system (all from Applied Biosystems, Carlsbad, CA, USA) under the following amplification conditions: denaturation, one cycle of 95 °C for 20 s, followed by 40 cycles each of 95 °C for 1 s and 60 °C for 20 s. Relative fold difference was quantified by the comparative Ct method normalized to 18 S rRNA and presented relative to the contralateral control (Livak and Schmittgen, 2001).

Immunofluorescence

Whole mounts of plantaris muscles were harvested ipsilateral and contralateral to transection injury in both wild-type and TCF/Lef:H2B-GFP ($n = 5$) mice as previously described (Chao et al., 2013). Immunofluorescent stainings were performed following 4% paraformaldehyde fixation with the following primary antibodies: active β-catenin (1:200); neurofilament 70 kDa (1:400; both from Millipore, Billerica, MA, USA), neurofilament (SMI-312, 1:400), Wnt3a (1:400; both from Abcam, Cambridge, MA, USA), synaptophysin (1:1), and Alexa 555-conjugated alpha-bungarotoxin (1:1,000; both from Invitrogen). Donkey anti-mouse IgG conjugated to Alexa 350 or 488, and donkey anti-rabbit IgG conjugated to Alexa 488 or 633 (1:500; Molecular Probes, Eugene, OR, USA) were used where appropriate for detection of primary antibodies. Images were acquired via confocal microscopy (LSM780, Zeiss, Jena, Germany).

Counting of GFP-positive cells

Images of plantaris muscles were captured as a Z-stack at 4× magnification to ensure visualization of the entire motor endplate band. Once the motor endplate band was visualized, VisioPharm software was utilized to select the motor endplate band through mask and grid creation. A filter was utilized to detect Alexa555 and VisioPharm selected the motor endplate band as characterized by fluorescence of Alexa555. Using VisioPharm's randomized selection, four images were randomly chosen *from* the motor endplate band at 20×. These 20× images of the Z-stack capture were then counted for their GFP-positive nuclei in that plane. They were then counted for the number of GFP-positive cells using ImageJ (NIH) software. This technique was again repeated to but selecting for the muscle outside of the motor endplate band as well.

Immunoblotting

Whole gastroc–soleus complex lysates were harvested from wild-type ($n = 9$) and TCF/Lef:H2B-GF mice ($n = 5$). Lysate protein concentration was determined using a BCA protein assay kit (Thermo Scientific). Samples were resolved on either 7.5% gels or 4–15% gels (Mini-Protean TGX precast gel; Bio-Rad, Hercules, CA, USA), and transferred to nitrocellulose membranes, blocked with 5% dry skimmed milk, and incubated overnight at 4 °C with the following primary antibodies diluted in 3% milk as indicated: green fluorescent protein (GFP, 1:1000; Molecular Probes), active β-catenin (1:1000; Millipore), and total β-catenin (1:1000; BD Biosciences, San Jose, CA, USA). For detection, goat anti-mouse or goat anti-rabbit secondary antibody conjugated with horseradish peroxidase (HRP; 1:5,000 dilution; Millipore) was used. Blots were developed with Western Chemiluminescent HRP Substrate (Thermo Scientific). Glyceraldehyde-3-phosphate dehydrogenase served as internal control when appropriate. The densitometric quantification of immunoblotting was carried out with Image Studio software (version 3.1; Li-Cor Biosciences, Lincoln, NE, USA).

Statistical analysis

Data are presented as mean ± standard error of the mean. A Two way analysis of variance with Bonferroni correction or two-tailed paired t-test was performed unless otherwise indicated. Statistical significance is reported as $p < 0.05$. Data analysis was carried out using SPSS v21 (IBM, Armonk, NY, USA).

RESULTS

Canonical Wnt signaling expression is increased after denervation injury in skeletal muscle

Wnt3a and Wnt3 mRNA levels were quantified through qRT-PCR to determine if NMJ destabilization is associated with changes in expression of these transcripts following traumatic nerve injury. The expression of Wnt3a mRNA was significantly increased by 2 weeks post-injury (2.8-fold increase over control; $p = 0.002$; Fig. 1A). Levels of Wnt3a transcripts were shown to increase steadily until 1 month post-injury, then, began decreasing thereafter (5.6-fold; $p < 0.001$; Fig. 1A). Conversely, sciatic nerve transection induced a decrease in the amount of non-canonical Wnt3 mRNA expression in denervated muscles relative to control at each time point. At 1 week, the decrease was most dramatic compared to control levels (0.06-fold; $p < 0.001$; Fig. 1A). Wnt3 mRNA levels gradually increased until 2 months after denervation, yet, still did not reach baseline levels (0.48-fold; $p < 0.001$; Fig. 1A). Thus, the negative regulator Wnt3a may play a role in NMJ destabilization following traumatic nerve injury.

The Wnt/β-catenin signaling pathway is activated after traumatic nerve injury

Immunohistochemistry of wild-type plantaris muscles demonstrated that Wnt3a was upregulated and recruited to the post-synaptic muscle (Fig. 1B). Interestingly, Wnt3a was seen to be preferentially localizing near degrading AChRs (Fig. 1B). Compared to denervated muscle, there was very minimal staining of Wnt3a in uninjured muscle.

Coinciding with Wnt3a upregulation, immunohistochemistry for active β-catenin is dramatically increased in the post-synaptic muscle as well (Fig. 2A, B).

As Wnt3a is a canonical Wnt that signals through β-catenin, we measured levels of activated β-catenin also. As expected, immunoblot data demonstrated that the ratio of active to total β-catenin protein level is elevated nearly twofold at 2 months post-injury as compared to controls (0.0252 ± 0.0057 vs. 0.0470 ± 0.0082; $p = 0.022$; Fig. 2C).

Wnt/β-catenin signaling pathway is activated preferentially near the destabilizing motor endplate band

Utilizing a Wnt reporter mouse, we sought to determine where the activation of β-catenin signaling was localized after denervation. Uninjured TCF/Lef:H2B-GFP plantaris muscles were shown to have a baseline activation of GFP throughout the motor endplate band (Fig. 3A). However, in the 1-month denervated muscles, the number of GFP-positive cells was significantly increased above these baseline levels near the degenerating AChRs along the motor endplate ($95.8 \pm 13.4/mm^2$ vs. $218.8 \pm 31.9/mm^2$, $p = 0.012$; Fig. 3C). Of note, very few GFP-positive cells were seen outside of the motor endplate band in *both* uninjured and denervated muscles ($3.8 \pm 2.8/mm^2$ vs. $2.8 \pm 1.6/mm^2$; Fig. 3B, D, E). Supportively, immunoblot analysis for GFP in the gastroc–soleus complexes shows an increase in the 1-month denervated muscle from TCF/Lef:H2B-GFP mice as compared to control (0.467 ± 0.037 vs. 1.636 ± 0.211, $p = 0.04$; Fig. 3F). These data suggest activation of the Wnt/β-catenin signaling cascade after traumatic nerve injury and its preferential localization near the degrading motor endplate band.

DISCUSSION

Our data reveal that Wnt3a mRNA and protein, as well as active β-catenin levels are increased in denervated muscles. Changes in the protein levels of Wnt3a and active β-catenin are closely associated with destabilization of the motor endplate. Furthermore, Wnt signaling activity, as detailed with the use of a novel transgenic mouse line, is observed preferentially localized at the degrading motor endplate band. These data support our hypothesis that the Wnt/β-catenin signaling pathway is involved in post-synaptic AChR destabilization after denervation injury.

Although the mechanism remains unclear, β-catenin has been reported to directly interact with rapsyn gene expression and reduce its downstream signaling (Zhang et al., 2007; Wang et al., 2008). Previously reported data have shown that denervated AChRs in adult animal models gradually disassemble (Hartzell and Fambrough, 1972; Frank et al., 1975; Steinbach, 1981). Furthermore, upregulation of β-catenin in cultured myotubes has been reported to inhibit agrin-induced AChR clustering, thus, suggesting its role as a negative regulator in NMJ formation (Wang et al., 2008). Moreover, expressing Wnt3a or β-catenin in the limb muscles of mice causes disassembly of AChR clusters (Wang et al., 2008). β-catenin may play a role in the disassembly of mature AChR clusters in denervated muscles by interacting with rapsyn. In an *in vivo* study utilizing agrin-deficient mice, it was shown that in the absence of agrin, AChR clusters were distributed in a wider pattern across the muscle (Gautam et al., 1996). Additionally, a recent study of NMJs in β-catenin gain of function

muscles revealed that the motor endplate band is also distributed in a wider pattern (Wu et al., 2012). Thus, we hypothesize that β-catenin may also contribute to the dispersion of AChR clusters after chronic denervation. Here, we have shown that β-catenin is upregulated near degrading and destabilized AChR clusters.

Interestingly, previous studies of Wnt expression are mostly reserved for tissues with high turnover, such as those of epithelial origin. However, our study revealed activation of Wnts in muscles, which has low turnover (Taipale and Beachy, 2001). These signals were observed only near the degrading AChRs and similar levels of GFP signal were not seen in other areas of the denervated muscle. Combined with previous evidence that the Wnt/β-catenin signaling pathway has a negative effect on the organization of the NMJ during development, these data provide supportive evidence that Wnt signaling may contribute to destabilization of the motor endplate following transection injury.

Recent advancements and studies have shown that the Wnt/β-catenin signaling cascade plays a crucial role in tumor biology (Polakis, 2012). This pathway is regulated at different levels by a wide range of antagonists, such as Dickkopf-related protein1, secreted Frizzled-related proteins, and Wnt inhibitory factor-1 (Cruciat and Niehrs, 2013). Genes for these secreted Wnt antagonists reported to be downregulated or inactivated in human cancers (Suzuki et al., 2004; Taniguchi et al., 2005; Aguilera et al., 2006; Veeck et al., 2006). Therefore, overexpression or administration of Wnt antagonists has shown to reduce *in vivo* tumor growth (Bafico et al., 2004; DeAlmeida et al., 2007). These results allow for the possibility of capitalizing on Wnt signal blockers that have been developed for cancer therapeutics to stabilize the NMJ after transection injury in the future. Combined with previous evidence that preservation of the motor endplate significantly enhances regeneration and functional recovery, these data suggest that targeting the Wnt/β-catenin pathway may offer a therapeutic opportunity for more effective and efficient reinnervation of end-plates to improve functional recovery.

CONCLUSION

This study demonstrated that Wnt3a is upregulated and β-catenin is activated following traumatic nerve injury, thus, suggesting a role for this pathway in NMJ destabilization. The Wnt/β-catenin signaling pathway may be a useful therapeutic target to prevent the motor endplate degeneration that occurs following traumatic nerve injury. Future directions include treatment with Wnt inhibitors as a pharmacologic adjunct to surgical repair.

Acknowledgments

Abbreviations

AChR	acetylcholine receptor
MMP3	matrix metalloproteinase-3
MuSK	muscle-specific kinase

NMJ	neuromuscular junction
qRT-PCR	quantitative real-time PCR
TCF	transgenic mouse line

References

Aguilera O, Fraga MF, Ballestar E, Paz MF, Herranz M, Espada J, García JM, Muñoz A, Esteller M, González-Sancho JM. Epigenetic inactivation of the Wnt antagonist DICKKOPF-1 (DKK-1) gene in human colorectal cancer. Oncogene. 2006; 25:4116–4121. [PubMed: 16491118]

Bafico A, Liu G, Goldin L, Harris V, Aaronson SA. An autocrine mechanism for constitutive Wnt pathway activation in human cancer cells. Cancer Cell. 2004; 6:497–506. [PubMed: 15542433]

Bentolila V, Nizard R, Bizot P, Sedel L. Complete traumatic brachial plexus palsy. Treatment and outcome after repair. J Bone Joint Surg Am. 1999; 81:20–28. [PubMed: 9973050]

Bezakova G, Helm JP, Francolini M, Lømo T. Effects of purified recombinant neural and muscle agrin on skeletal muscle fibers in vivo. J Cell Biol. 2001; 153:1441–1452. [PubMed: 11425874]

Chao T, Frump D, Lin M, Caiozzo VJ, Mozaffar T, Steward O, Gupta R. Matrix metalloproteinase 3 deletion preserves denervated motor endplates after traumatic nerve injury. Ann Neurol. 2013; 73:210–223. [PubMed: 23281061]

Clevers H, Nusse R. Wnt/β-catenin signaling and disease. Cell. 2012; 149:1192–1205. [PubMed: 22682243]

Cruciat C-M, Niehrs C. Secreted and transmembrane wnt inhibitors and activators. Cold Spring Harb Perspect Biol. 2013; 5:a015081. [PubMed: 23085770]

DeAlmeida VI, Miao L, Ernst JA, Koeppen H, Polakis P, Rubinfeld B. The soluble wnt receptor Frizzled8CRD-hFc inhibits the growth of teratocarcinomas in vivo. Cancer Res. 2007; 67:5371–5379. [PubMed: 17545618]

Ferrer-Vaquer A, Piliszek A, Tian G, Aho RJ, Dufort D, Hadjantonakis A-K. A sensitive and bright single-cell resolution live imaging reporter of Wnt/ß-catenin signaling in the mouse. BMC Dev Biol. 2010; 10:121. [PubMed: 21176145]

Frank E, Gautvik K, Sommerschild H. Cholinergic receptors at denervated mammalian motor end-plates. Acta Physiol Scand. 1975; 95:66–76. [PubMed: 1180105]

Gautam M, Noakes PG, Moscoso L, Rupp F, Scheller RH, Merlie JP, Sanes JR. Defective neuromuscular synaptogenesis in agrin-deficient mutant mice. Cell. 1996; 85:525–535. [PubMed: 8653788]

Griffin JW, Hogan MV, Chhabra AB, Deal DN. Peripheral nerve repair and reconstruction. J Bone Joint Surg Am. 2013; 95:2144–2151. [PubMed: 24306702]

Hartzell HC, Fambrough DM. Acetylcholine receptors. Distribution and extrajunctional density in rat diaphragm after denervation correlated with acetylcholine sensitivity. J Gen Physiol. 1972; 60:248–262. [PubMed: 5055788]

Henríquez JP, Salinas PC. Dual roles for Wnt signalling during the formation of the vertebrate neuromuscular junction. Acta Physiol (Oxf). 2012; 204:128–136. [PubMed: 21554559]

Henriquez JP, Webb A, Bence M, Bildsoe H, Sahores M, Hughes SM, Salinas PC. Wnt signaling promotes AChR aggregation at the neuromuscular synapse in collaboration with agrin. Proc Natl Acad Sci U S A. 2008; 105:18812–18817. [PubMed: 19020093]

Kang JR, Zamorano DP, Gupta R. Limb salvage with major nerve injury: current management and future directions. J Am Acad Orthop Surg. 2011; 19(Suppl 1):S28–S34. [PubMed: 21304044]

Kim DH, Cho Y-J, Tiel RL, Kline DG. Outcomes of surgery in 1019 brachial plexus lesions treated at Louisiana State University Health Sciences Center. J Neurosurg. 2003; 98:1005–1016. [PubMed: 12744360]

Koles K, Budnik V. Wnt signaling in neuromuscular junction development. Cold Spring Harb Perspect Biol. 2012:4.

Li VSW, Ng SS, Boersema PJ, Low TY, Karthaus WR, Gerlach JP, Mohammed S, Heck AJR, Maurice MM, Mahmoudi T, Clevers H. Wnt signaling through inhibition of β-catenin degradation in an intact Axin1 complex. Cell. 2012; 149:1245–1256. [PubMed: 22682247]

Lin W, Dominguez B, Yang J, Aryal P, Brandon EP, Gage FH, Lee K-F. Neurotransmitter acetylcholine negatively regulates neuromuscular synapse formation by a Cdk5-dependent mechanism. Neuron. 2005; 46:569–579. [PubMed: 15944126]

Livak KJ, Schmittgen TD. Analysis of relative gene expression data using real-time quantitative PCR and the 2(−Delta Delta C(T)) Method. Methods. 2001; 25:402–408. [PubMed: 11846609]

McMahan UJ. The agrin hypothesis. Cold Spring Harb Symp Quant Biol. 1990; 55:407–418. [PubMed: 1966767]

Moon RT, Bowerman B, Boutros M, Perrimon N. The promise and perils of Wnt signaling through beta-catenin. Science. 2002; 296:1644–1646. [PubMed: 12040179]

Niehrs C. The complex world of WNT receptor signalling. Nat Rev Mol Cell Biol. 2012; 13:767–779. [PubMed: 23151663]

Polakis P. Wnt signaling in cancer. Cold Spring Harb Perspect Biol. 2012:4.

Ray WZ, Mackinnon SE. Management of nerve gaps: autografts, allografts, nerve transfers, and end-to-side neurorrhaphy. Exp Neurol. 2010; 223:77–85. [PubMed: 19348799]

Samuel MA, Valdez G, Tapia JC, Lichtman JW, Sanes JR. Agrin and synaptic laminin are required to maintain adult neuromuscular junctions. PLoS One. 2012; 7:e46663. [PubMed: 23056392]

Seddon HJ, Medawar PB, Smith H. Rate of regeneration of peripheral nerves in man. J Physiol. 1943; 102:191–215. [PubMed: 16991601]

Steinbach JH. Neuromuscular junctions and alpha-bungarotoxin-binding sites in denervated and contralateral cat skeletal muscles. J Physiol. 1981; 313:513–528. [PubMed: 7277234]

Suzuki H, Watkins DN, Jair K-W, Schuebel KE, Markowitz SD, Chen WD, Pretlow TP, Yang B, Akiyama Y, Van Engeland M, Toyota M, Tokino T, Hinoda Y, Imai K, Herman JG, Baylin SB. Epigenetic inactivation of SFRP genes allows constitutive WNT signaling in colorectal cancer. Nat Genet. 2004; 36:417–422. [PubMed: 15034581]

Taipale J, Beachy PA. The Hedgehog and Wnt signalling pathways in cancer. Nature. 2001; 411:349–354. [PubMed: 11357142]

Takamori M. Structure of the neuromuscular junction: function and cooperative mechanisms in the synapse. Ann N Y Acad Sci. 2012; 1274:14–23. [PubMed: 23252893]

Taniguchi H, Yamamoto H, Hirata T, Miyamoto N, Oki M, Nosho K, Adachi Y, Endo T, Imai K, Shinomura Y. Frequent epigenetic inactivation of Wnt inhibitory factor-1 in human gastrointestinal cancers. Oncogene. 2005; 24:7946–7952. [PubMed: 16007117]

Tung TH, Mackinnon SE. Nerve transfers: indications, techniques, and outcomes. J Hand Surg Am. 2010; 35:332–341. [PubMed: 20141906]

Valenzuela DM, Stitt TN, DiStefano PS, Rojas E, Mattsson K, Compton DL, Nuñez L, Park JS, Stark JL, Gies DR. Receptor tyrosine kinase specific for the skeletal muscle lineage: expression in embryonic muscle, at the neuromuscular junction, and after injury. Neuron. 1995; 15:573–584. [PubMed: 7546737]

Veeck J, Niederacher D, An H, Klopocki E, Wiesmann F, Betz B, Galm O, Camara O, Dürst M, Kristiansen G, Huszka C, Knüchel R, Dahl E. Aberrant methylation of the Wnt antagonist SFRP1 in breast cancer is associated with unfavourable prognosis. Oncogene. 2006; 25:3479–3488. [PubMed: 16449975]

Wang J, Ruan N-J, Qian L, Lei W, Chen F, Luo Z-G. Wnt/beta-catenin signaling suppresses Rapsyn expression and inhibits acetylcholine receptor clustering at the neuromuscular junction. J Biol Chem. 2008; 283:21668–21675. [PubMed: 18541538]

Wu H, Lu Y, Barik A, Joseph A, Taketo MM, Xiong W-C, Mei L. β-Catenin gain of function in muscles impairs neuromuscular junction formation. Development. 2012; 139:2392–2404. [PubMed: 22627288]

Zhang B, Luo S, Dong X-P, Zhang X, Liu C, Luo Z, Xiong W-C, Mei L. Beta-catenin regulates acetylcholine receptor clustering in muscle cells through interaction with rapsyn. J Neurosci. 2007; 27:3968–3973. [PubMed: 17428970]

Zhang B, Luo S, Wang Q, Suzuki T, Xiong WC, Mei L. LRP4 serves as a coreceptor of agrin. Neuron. 2008; 60:285–297. [PubMed: 18957220]
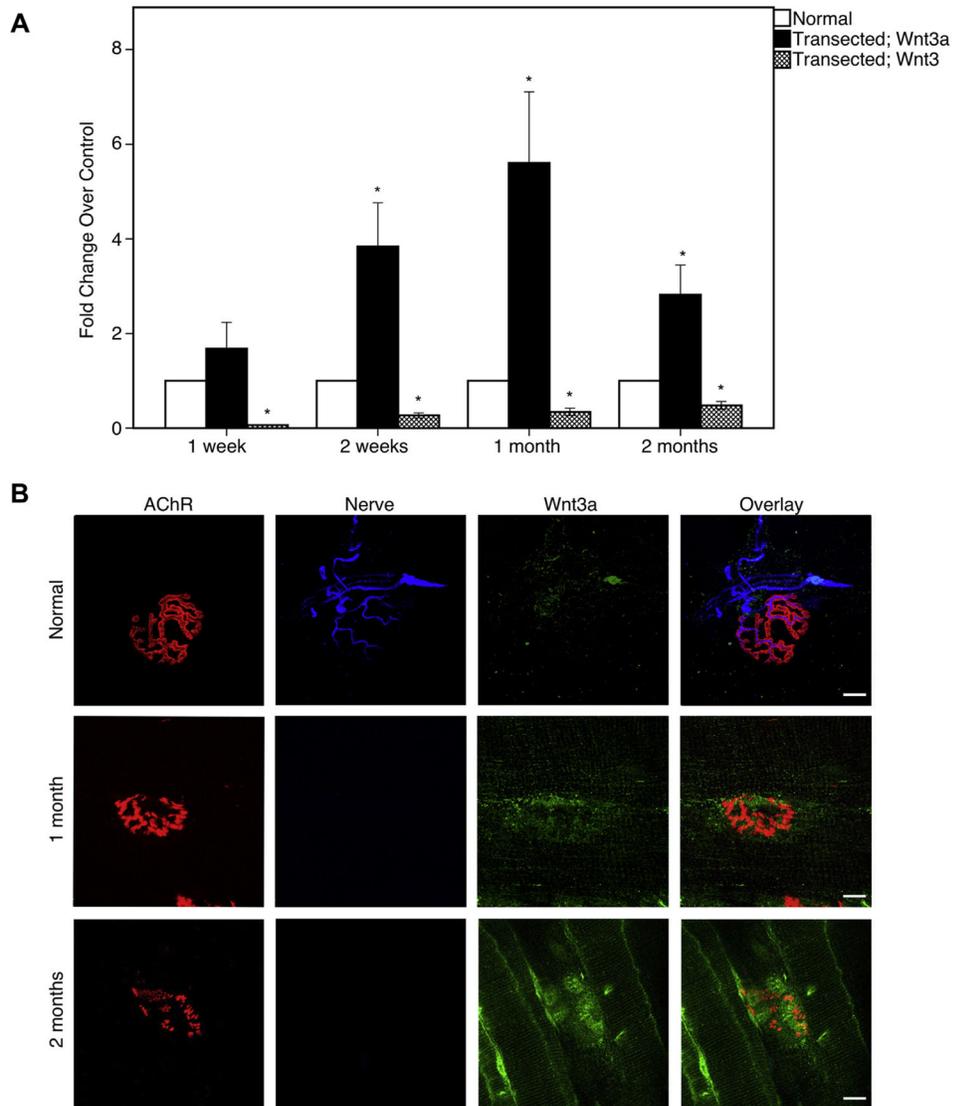
Fig. 1.
Wnt3a expression in denervated muscles. (A) qRT-PCR of Wnt3a and Wnt3 in at different timepoints after denervation injury. Wnt3a is elevated at 2 weeks to 2 months. However, Wnt3, a non-canonical Wnt, is decreased during this time. (B) Wnt3a is co-localized to the nerves in uninjured mice. After denervation injury, Wnt3a is upregulated. Wnt3a expression is localized at the post-synaptic muscle, preferentially at the sites of degenerating AChRs which are no longer innervated. Bar graphs represent mean ± S.E. ($n = 7$ per group). $^*p < 0.05$. Red = α-bungarotoxin; blue = neurofilament; green = Wnt3a. Scale bar = 10 μm (100×). (For interpretation of the references to color in this figure legend, the reader is referred to the web version of this article.)
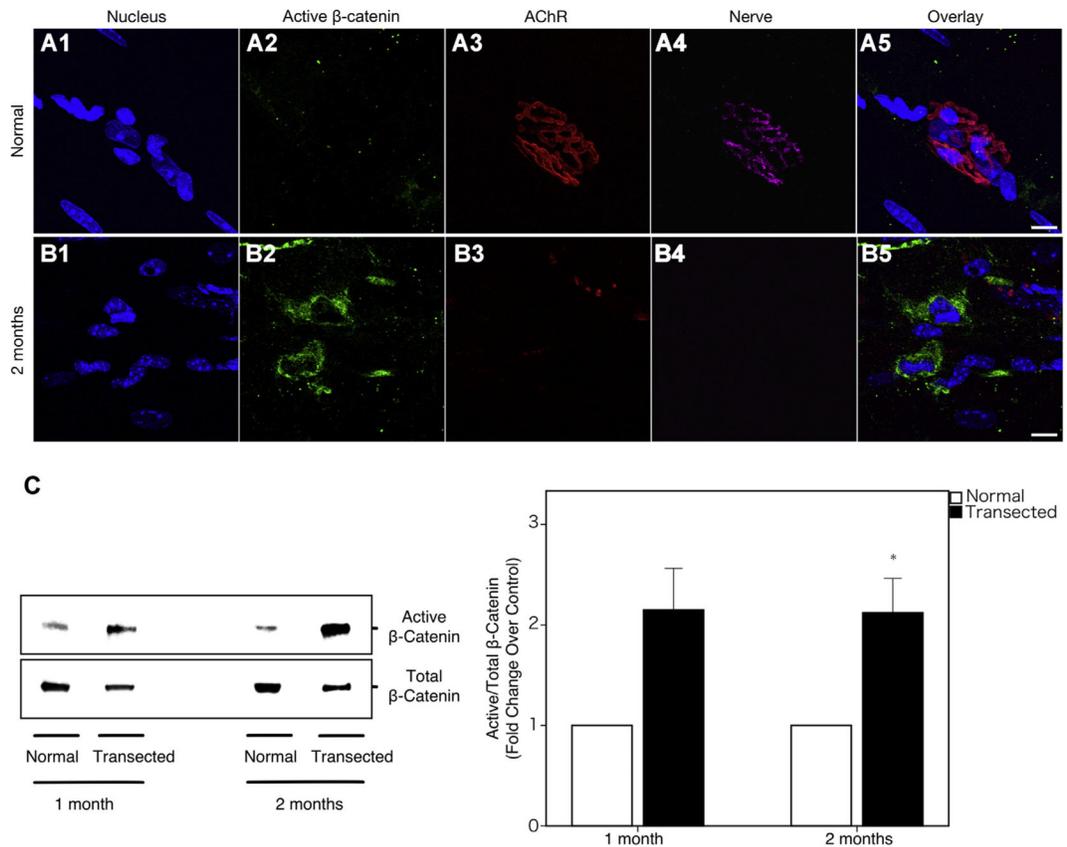
Fig. 2.
β-catenin activity in plantaris muscles 2 months post-transection. (A1–A5) Uninjured wild-type muscles do not have inherent β-catenin activity. (B1–B5). However, after 2 months denervation injury is introduced, β-catenin is dramatically increased in the post-synaptic muscle. (C) Immunoblot analysis demonstrated that the ratio of active/total β-catenin protein level is nearly twofold elevated in the 2-month denervated muscle as compared to control, signifying activation of the Wnt/β-catenin signaling pathway. Blue = DAPI; green = active β-catenin; red = α-bungarotoxin; purple = synaptophysin. Scale bar = 10 μm (100×). Bar graphs represent mean ± S.E. ($n = 9$ per group). $^{*}p < 0.05$. (For interpretation of the references to color in this figure legend, the reader is referred to the web version of this article.)
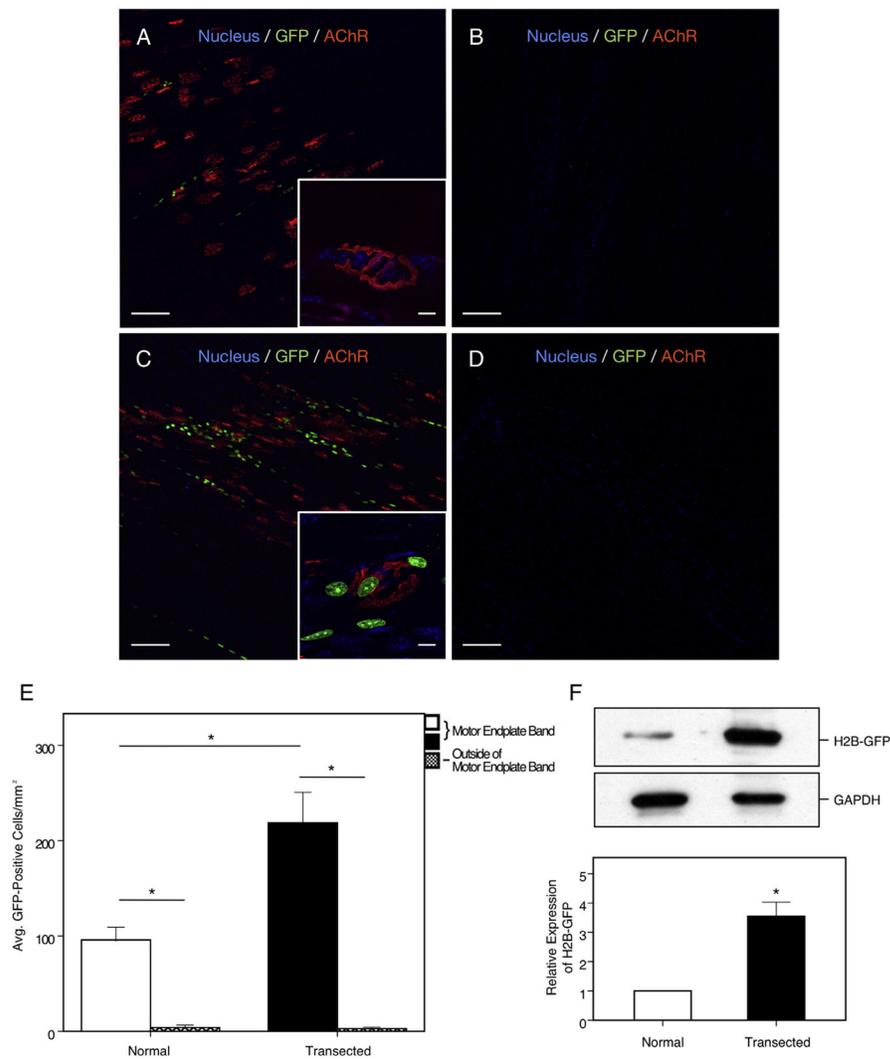
Fig. 3.
H2B-GFP expression in plantaris muscles after 1 month denervation. (A, B) Sham-operated muscles show minimal GFP fluorescence at the motor endplate band with no fluorescence seen at other sites of the muscle. Inset shows a magnified AChR with absent GFP fluorescence, signifying minimal Wnt activity at baseline. (C, D) One month denervated muscles show significantly elevated GFP fluorescence and Wnt activity but similar signaling was not seen outside of the motor endplate band. Inset shows AChR with multiple GFP histones fluorescing. (E) Total number of GFP-positive cells counted at the motor endplate band and outside of the motor endplate in sham-operated and 1-month denervated muscle. (F) Immunoblot analysis probed for GFP showing a relative increase of nearly threefold in the 1-month denervated muscle as compared to control. Green = GFP; red = α-bungarotoxin; blue = DAPI. Scale bars = 100 μm (10×), 10 μm (100×). Bar graphs represent mean ± S.E. ($n = 5$ per group). $^{*}p < 0.05$. (For interpretation of the references to color in this figure legend, the reader is referred to the web version of this article.)